

## **Vortex-acoustic lock-on in bluff-body and backward-facing step combustors**

S R CHAKRAVARTHY<sup>1</sup>, R SIVAKUMAR<sup>2</sup> and  
O J SHREENIVASAN<sup>1</sup>

<sup>1</sup>Department of Aerospace Engineering and

<sup>2</sup>Department of Mechanical Engineering, Indian Institute of Technology –  
Madras, Chennai 600 036

e-mail: src@ae.iitm.ac.in

**Abstract.** Experimental data on acoustic pressure measurements obtained over a wide range of conditions is reported for two simple geometries that are commonly studied for their combustion dynamics behaviour. These geometries are the confined bluff-body and the confined backward-facing steps. The data indicate regimes of flow-acoustic lock-on that signifies the onset of combustion instability, marked by the excitation of high-amplitude discrete tones of sound in the combustor. The high-speed chemiluminescence imaging of the combustion zone indicates heat-release-rate fluctuations occurring at the same frequencies as observed in the acoustic spectra. Attention is then devoted to the data obtained under cold-flow conditions to illustrate distinctly different behaviour than when combustion instability occurs, contrary to the commonly held view that the combustion process does not alter the underlying fluid mechanical processes under low-Mach number conditions.

**Keywords.** Combustion instability; backward-facing step; bluff-body; acoustic field; vortex-acoustic lock-on; chemiluminescence.

### **1. Introduction**

Combustion dynamics is an area that is still not very well understood despite decades of work on it. This is borne out by two features: (a) even today, an engineer in the industry does not have any reliable theoretical approach to confidently predict or control unstable operating regimes of engines, (b) the subject is highly inter-disciplinary in nature. Combustion dynamics involves three disciplines, namely, combustion, fluid mechanics, and acoustics. Strictly, all of it is fluid mechanics, but the first and last disciplines certainly have specific features that mark them out from mainstream fluid-mechanics, which by itself has a central role to play. The purpose of this paper is to highlight the fluid mechanical aspect of combustion dynamics and the need for diagnostics to resolve some questions that arise from the results presented here.

One of the important driving mechanisms of combustion instability has been that due to vortex-shedding, as highlighted by Schadow & Gutmark (1992), who showed that the development of coherent flow structures and their breakdown into fine-scale turbulence can lead

to periodic heat-release. Many workers have investigated combustor geometries that include a predominant role for vortex-shedding, such as dump combustors involving axisymmetric backward-facing step (Poinsot *et al* 1987; Sivasegaram & Whitelaw 1987; Gutmark *et al* 1991; Sterling & Zukowski 1991; Yu *et al* 1991) and bluff-body flame-holders (Hegde *et al* 1987; Langhorne 1988; Macquistein & Dowling 1993). They have deduced the phase relationship between the vortex roll-up sequence and the heat-release fluctuations under conditions of excitation of intense oscillations.

Lieuwen (2002) has also reported experimental characterization of limit-cycle oscillations in a premixed dump combustor, including examples of transition from stable to unstable combustor operation in the form of supercritical and sub-critical bifurcations.

Almost all the studies on combustion instability focus on investigations under conditions when the combustion oscillations are unstable. With the sole exception of Lieuwen (2002) recently, there has been no systematic work on the wide variation of geometric parameters of the combustor and flow conditions that ranges from a regime of low-intensity noise generation without appreciable acoustic feedback from the combustion chamber on the combustion process, to a regime of excitation of high-intensity discrete tones symptomatic of combustion instability. The Rayleigh criterion delineates regimes of unstable combustion from those of stable combustion, but this is only a necessary condition that could be met by a variety and combination of physical mechanisms. Such mechanisms would gradually vary in predominance and interplay with one another, leading to a transition from low-amplitude noise to high-amplitude instability conditions. A systematic variation would prompt investigation on the mechanisms that dictate the onset of instability. The data can also serve to identify precursors to instability that can be utilized in actively deploying certain passive control measures in practical combustion systems.

The present paper reports some experimental data obtained in this laboratory on two combustor geometries most commonly studied by past investigators, i.e., the bluff-body combustor and the backward-facing step combustor. The data are obtained over a wide range of combustion conditions from those at which low-amplitude broadband acoustic oscillations are excited to those when intense discrete tones are excited. The corresponding cold-flow conditions do not involve excitation of high-amplitude oscillations, but the trends in the dominant frequencies do indicate an unsteady flow behaviour that is very different from that under the combustion conditions, particularly when the intense discrete tones are observed. The objective of this paper is to highlight this disparity.

The commonly held view of the role of fluid flow in combustion is that it is altered by a decrease in density due to the heat-release in the combustion zone. Mostly, this does not imply qualitatively different behaviour of the flow field under combustion conditions than under cold-flow conditions, when the mean Mach number of the flow is very low, as commonly encountered. However, when interacting with the self-excited acoustic oscillations as considered in the present paper, this does not appear to be the case.

## 2. Experimental set-ups

As mentioned earlier, two geometries are considered here: the confined bluff-body and the confined backward-facing step. Methane is used as fuel in both cases.

Figure 1 shows the experimental set-up for the confined bluff-body. It is a rectangular geometry of constant width 25 mm and constant height 62 mm, downstream of the settling chamber, to provide access for optical diagnostic investigation. The test section contains the

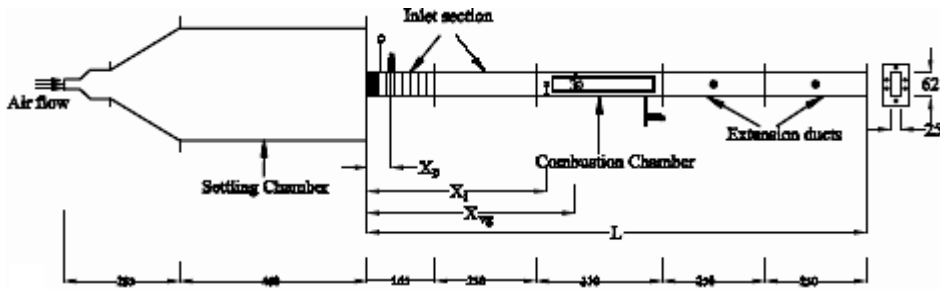


Figure 1. Schematic of the confined bluff-body set-up.

bluff-body in the form of a V-gutter with an included angle of  $90^\circ$ . The fuel is injected through a slit running across the 25 mm width of the test section in a circular injector manifold of 6 mm outer diameter, upstream of the bluff-body. The distance between the fuel-injection manifold and the bluff-body can be varied in three steps.

Figure 2 shows the experimental set-up for the confined backward-facing step. It is also a rectangular geometry of constant width 60 mm, downstream of the settling chamber. The test section contains the backward-facing step, whose height has been maintained at 30 mm in the present study. Provision is made for injection of the fuel below the top edge of the step.

In both geometries, the total length of the duct can be varied with the use of extension ducts, both upstream and downstream of the test section. In the first case, the extension ducts are of equal size, both upstream and downstream of the test section, but are of different heights in the second case. The axial location of the test section is also varied along the total length of the combustor in both cases.

### 3. Acoustic measurements under combustion conditions

The dominant frequency in the spectra recorded by transducers mounted in the ports at different axial locations along the length of the set-up is plotted in terms of the Helmholtz number, defined as  $He = fL/c$ , where  $c$  is the speed of sound under reference conditions at the inlet. A constant Helmholtz number indicates a duct acoustic mode, but a linear variation with Reynolds number indicates that the recorded frequency corresponds to vortex-shedding.

#### 3.1 Confined bluff-body geometry

Figure 3 shows the Helmholtz number variation with Reynolds number for the confined bluff-body geometry with duct length  $L/h = 92.19$  for two different axial locations of the bluff-body (V-gutter). It can be seen in figure 3a that, up to  $Re \approx 27000$ , the different locations

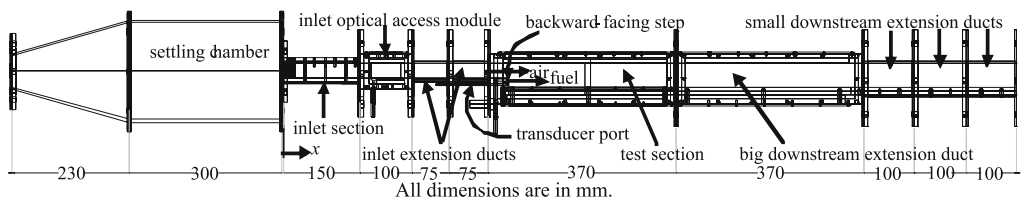
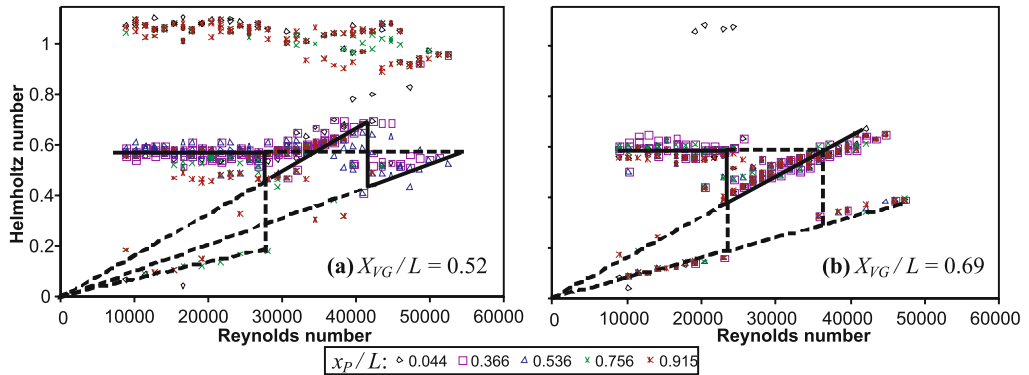


Figure 2. Schematic of the confined backward-facing step set-up.



**Figure 3.** Observed dominant frequency at many fuel-flow rates for the confined bluff-body with  $L/h = 92.19$ .

in the duct record different dominant frequencies, of which the fundamental acoustic mode is dominant in the middle. Above this, the fundamental acoustic mode is observed to exhibit a linear variation of a certain slope, followed by a jump to another straight line of a lower slope at a higher Reynolds number. However, as the bluff-body is located further upstream, as in figure 3b, the dominant frequencies at most transducer ports coincide, and the onset of transition from a constant Helmholtz number to a linearly increasing variation occurs at a lower Reynolds number than in the previous case. Also, no further transitions occur. Although not shown here in the interest of space, the amplitude levels reach a maximum for the second case at optimum fuel-flow rates, particularly at the onset of the transition from the constant to the linear variation. This transition marks a vortex-acoustic lock-on, wherein the natural acoustic mode of the duct shifts in a manner of the vortex-shedding variation with Reynolds number. This is the opposite of lock-on in the case of vortex-shedding in the wake-flow past vibrating bodies (Blevins 1990) or through an orifice in a duct (Karthik *et al* 2003, 2004), wherein the vortex-shedding frequency shifts in the manner of the natural frequency of vibration or the natural frequency of the acoustic mode of the duct, as the Reynolds number is increased in the lock-on regime. This distinction is schematically shown in figure 4.

The linear variation with different slopes indicates different modes of vortex-shedding, as in the possibility of vortex pairing or merging, resulting in a lower shedding frequency (lower Strouhal number) and consequently a lower slope, as in figure 3.

### 3.2 Confined backward-facing step geometry

Figure 5 shows the Helmholtz number variation with Reynolds number for the confined backward-facing step geometry at different fuel-flow rates and two lengths of the combustor. The measurement shown here was made at the backward-facing step. At the lower combustor length, multiple acoustic modes are observed to be excited at different fuel-flow rates, but the acoustic modes do not show linear variation under most of the test conditions, except perhaps for relatively high fuel-flow rates particularly at high Reynolds number. On the other hand, mostly one dominant acoustic mode is excited under most test conditions for the longer combustor length, which changes from a constant at low Reynolds numbers to several straight lines with non-zero decreasing slopes sequentially with increase in Reynolds numbers, the transition being governed by the fuel-flow rate level. The amplitude levels, not shown here, are quite low for the first case but quite high for the second case, particularly when transition

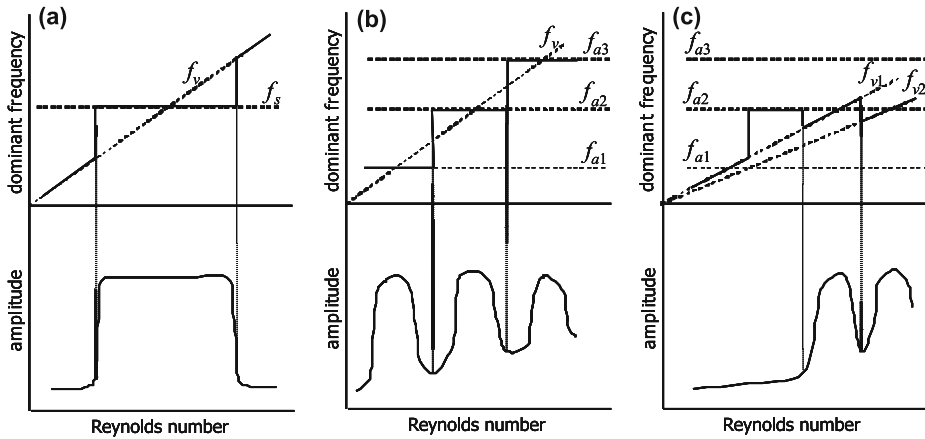


**Figure 4.** Schematic representation of qualitative variation of lock-on with vortex shedding encountered in different situations:  $f_v$  = vortex shedding frequency,  $f_s$  = natural frequency of structural vibration,  $f_a$  = natural acoustic mode frequency of duct. (a) Vortex–structure lock-on; (b) vortex–acoustic lock-on (cold flow); (c) vortex-acoustic lock-on (combustion).

from the constant to linear variation occurs for each fuel-flow rate, similar to what is observed with the previous geometry.

**4. Cold flow acoustic measurements**

Under cold-flow conditions within the test range of flow Reynolds numbers and bluff-body or backward-facing step length-scales, no vortex-acoustic lock-on is observed. Correspondingly, the acoustic amplitudes excited are at very low levels. Indeed, the vortex-acoustic lock-on observed under some conditions with combustion as seen in figures 3 and 5 is due to the effect of the oscillatory heat-release accompanying the vortex dynamics, which is absent under cold-flow conditions. One needs to keep this in mind in viewing the cold-flow results presented here.

**4.1 Confined bluff-body geometry**

Figure 6 shows the dominant frequencies measured under cold-flow conditions at different locations for the same two combustor configurations, both of the same length for the confined

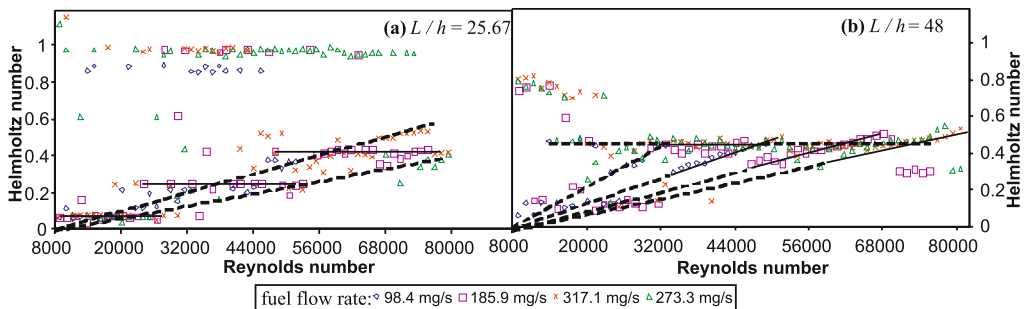


**Figure 5.** Observed dominant frequency at the step base for the confined backward-facing step.

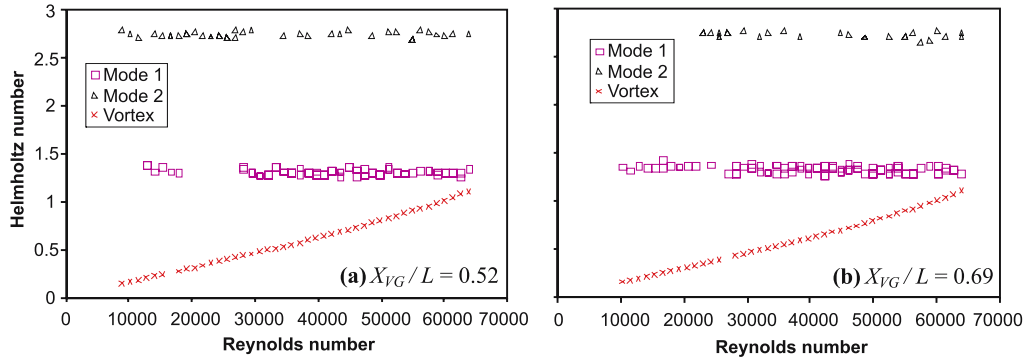


**Figure 6.** Observed dominant frequency under cold-flow conditions for confined bluff-body for  $L/h = 92.19$ .

bluff-body geometry, as in figure 3. Four out of the five locations of measurement record two different natural acoustic modes, i.e., constant Helmholtz numbers, but the measurement location just downstream of the bluff body in both configurations shows a linear variation of the Helmholtz number with Reynolds number. This clearly indicates that the pressure fluctuations due to vortex-shedding dominate over the acoustic-mode oscillations in the near-field of the bluff-body. This is also markedly different from the variation observed under combustion conditions in figure 3.

4.2 *Confined backward-facing step geometry*

Figure 7 shows the dominant frequencies measured at the step base under cold-flow conditions for the same configurations as those in figure 5 for the confined backward-facing step geometry. It can be seen that, unlike in the case of bluff-body under cold-flow conditions (figure 6), and also unlike in the case of combustion in the same backward-facing step geometry (figure 5), figure 7 does not show any variation in the dominant frequency exhibiting the behaviour of vortex-shedding, i.e., the linear variation of the Helmholtz number with Reynolds number. Such a variation is not the most dominant one and hence is not observed in figure 7. This could be due to a mere flapping of the shear layer (Driver *et al* 1987) originating from a single point of flow separation in the confined backward-facing

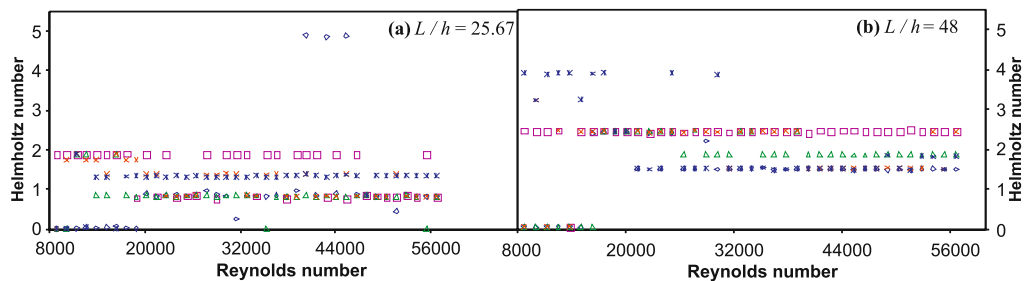


**Figure 7.** Observed dominant frequency at the step base under cold conditions for the confined backward-facing step.

step geometry, as opposed to the case of vortex roll-up from two points of separation in the bluff-body geometry. Hence, a stronger fluid mechanical pressure variation is sensed in the latter case. The flapping of the separating shear layer in the case of the backward-facing step is accompanied by Kelvin–Helmholtz instability leading to a relatively small-scale vortex roll-up in the near-field of the step, as opposed to the Karman vortex pattern in the other case.

## 5. High-speed chemiluminescence imaging

In order to resolve if, in the combustion situation, the heat-release-rate fluctuations indeed occur at the vortex-shedding frequency, high-speed imaging of the chemiluminescence in the combustion zone has been performed. The chemiluminescence of the  $\text{CH}^*$  radicals is obtained by use of an optical filter whose transmission peaks around a wavelength of 431 nm. A high-speed camera (HiSiS 2002, KSV Instruments, Finland) has been used for this purpose. The imaging is performed at a framing rate of 2250 fps for a duration of 3.6 s.

The sum of the chemiluminescent intensities at all the pixels in the field of view is obtained from each frame of the high-speed imaging, and the spectra of the total chemiluminescent intensity fluctuation is examined for its dominant frequencies in comparison with those obtained in the acoustic transducer measurements performed simultaneously. Since the wavelength of the acoustic oscillations is typically large when compared to the length-scale of the combustion zone, the total chemiluminescent intensity fluctuation can be taken to represent the total heat-release-rate fluctuation in the combustion zone, as if it is a compact source of sound. However, the summation over the entire field of view of imaging to obtain the total chemiluminescent intensity fluctuation causes a bias towards low-frequency oscillations, since the fluctuations associated with small-scale vortex roll-up, such as due to the Kelvin–Helmholtz instability in the flapping shear layer downstream of the backward-facing step, would be smeared out.

The results are shown in figure 8 for the case of the confined backward-facing step, before and after the onset of combustion–acoustic lock-on. It can be seen that the dominant frequencies in the total-chemiluminescent intensity and the acoustic spectra match exactly, indicating that the fluctuations in the heat-release-rate cause the acoustic pressure fluctuations at both conditions. However, as noted earlier, the dominant frequency of the pressure fluctuations everywhere in the duct follows the pattern of the vortex-shedding frequency after the onset of vortex-acoustic lock-on. This shows that the vortex-shedding process is responsible for the heat-release-rate fluctuations that drive the acoustic oscillations. The spectra before the onset of lock-on are broadband in nature and of low amplitude, in contrast to those after the onset of the lock-on, as expected. Moreover, despite the total chemiluminescent intensity fluctuation being always biased towards low frequencies, as mentioned earlier, the amplitude at the dominant acoustic frequency is found to be more significant in the total chemiluminescence spectra after the onset of lock-on, than before.

The unsteady pressure amplitudes measured in the cold-flow situation in both the geometries is considerably lower than during combustion, as mentioned earlier. This indicates that the vortex-induced sound generation and resonance is not a predominant mechanism when compared to that due to the fluctuating heat-release-rate during the combustion. However, it is the vortex dynamics that causes the heat-release-rate during combustion to fluctuate. This is

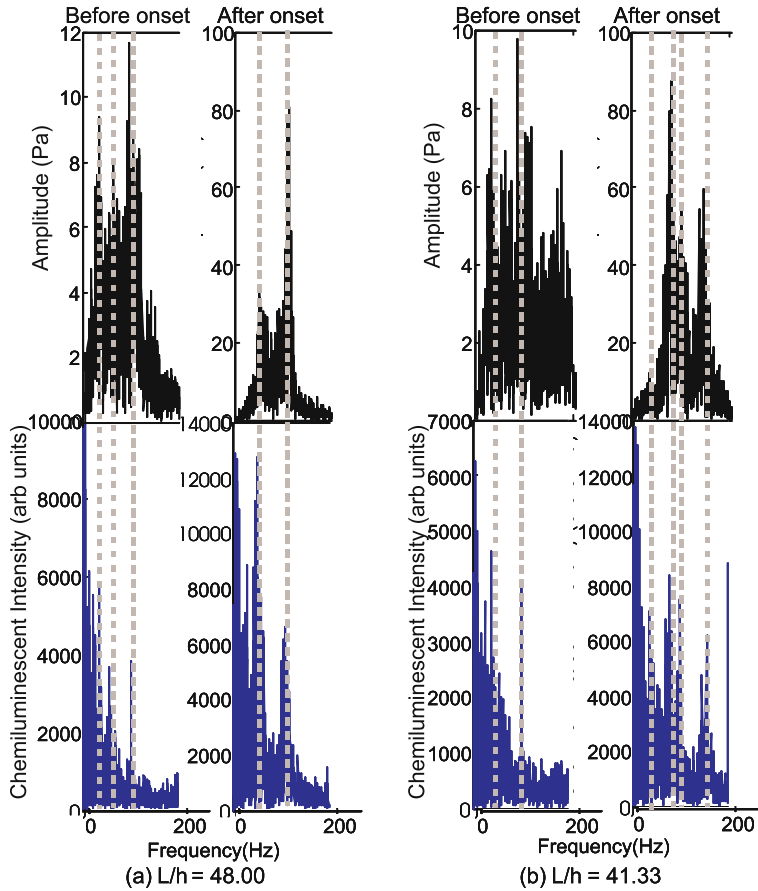


**Figure 8.** Comparison of acoustic and total chemiluminescent intensity spectra for the confined backward-facing step.

schematically depicted in figure 9 for both the combustor geometries considered in the present work. It is quite likely that the vortices are dilated due to periodic heat addition during combustion, which may promote their merger with increase in the Reynolds number, as observed with the decreasing slopes of the linear variation in the dominant frequency in the lock-on regime. Further, the density variation accompanying the heat addition causes the generation of baroclinic vorticity, which is usually of the opposite sense to that of the original vortex roll-up. This would influence the dynamics of the vortex roll-up at the flame stabilization location, and in turn, the fluctuating heat-release that excites the acoustic oscillations in the combustion case.

The above discussion highlights the need for further diagnostics of the flow field under cold-flow and combustion conditions to obtain the velocity and the vorticity fields. While the latter is afforded by particle image velocimetry, the former can be achieved in a time-resolved manner with the help of laser-Doppler velocimetry. These are currently being performed in this laboratory on both the geometries considered in this paper.

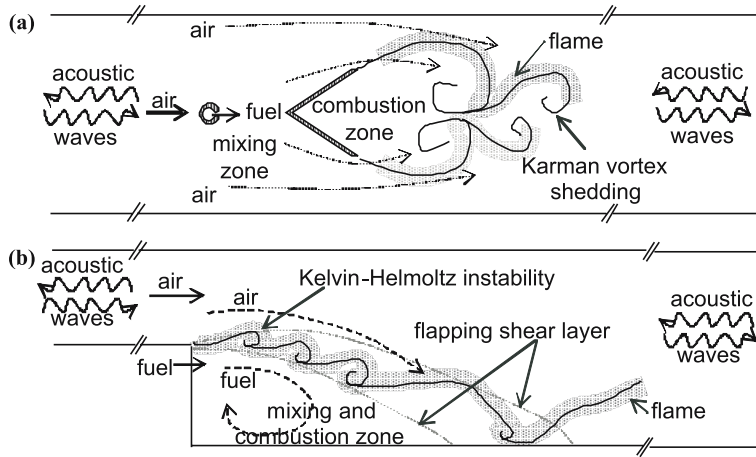


**Figure 9.** Schematic description of vortex-flame-acoustic interaction processes in (a) bluff-body combustor, (b) backward-facing step combustor.

## 6. Conclusion

It can be seen from the above results that the behaviour of the flow field under cold conditions is qualitatively different from those under combustion conditions of vortex-acoustic lock-on. The difference is not merely quantitative due to the dilating effect of the heat-release in the latter case, as is often considered. It is observed that the natural acoustic mode of the duct adjusts itself to varying in the manner of the vortex-shedding behaviour with Reynolds number under the lock-on conditions with the acoustic oscillations, which are driven by the fluctuating heat-release accompanying the vortex-shedding process during combustion. This is the opposite of the trend observed in cold-flow lock-on of vortex-shedding with natural frequency of vibration of bluff-bodies or natural frequency of acoustics of ducts with orifices, observed in the literature (figure 4). The presence of the confinement also alters the fluid mechanical behaviour even under cold conditions in contrast to what is usually reported in the literature for external flows.

The work highlights the need to understand the unsteady fluid mechanical behaviour in response to acoustic oscillations even under cold-flow conditions, possibly with the use of optical diagnostic techniques. This understanding would help explain the vortex-acoustic lock-on observed under combustion conditions, which marks the onset of combustion instability in practical systems. This is identified when a systematic variation of conditions ranging from the non-lock-on regime of low-amplitude broadband noise generation to the lock-on regime of excitation of high-amplitude discrete tones is undertaken. Such an approach to the study of combustion dynamics would enable the development of simple active deployment of passive-control measures based on detection of precursors to instability-like conditions.

We wish to dedicate this work to Dr P R Viswanath in appreciation of his services to fluid mechanics research in India. This work is partly funded by the Deutsche Forschungsgemeinschaft, Germany, and partly by the Aeronautical Research and Development Board, New Delhi.

**References**

- Blevins R D 1990 *Flow induced vibration* 2nd edn (New York: van Nostrand Reinhold)
- Driver D M, Seegmiller H L, Marvin J G 1987 *AIAA J.* 25: 914–919
- Gutmark E J, Schadow K C, Sivasegaram S, Whitelaw J H 1991 *Combust. Sci. Technol.* 79: 161–166
- Hegde U G, Reuter D, Zinn B T 1987 AIAA Paper No. 87–216
- Karthik B, Chakravarthy S R, Sujith R I 2003 *J. Acoust. Soc. Am.* 113: 2091–2094
- Karthik B, Venkateswarlu N, Kowsik B V R, Chakravarthy S R, Sujith R I, Tulapurkara E G 2004 *J. Aero. Soc. India* 56: 217–225
- Langhorne P J 1988 *J. Fluid Mech.* 193: 417–443
- Lieuwen T C 2002 *J. Propulsion* 18: 61–67
- Macquistein M A, Dowling A P 1993 *Combust. Flame* 94: 253–264
- Poinsot T J, Trouve A C, Veynante D P, Candel S M, Esposito E J 1987 *J. Fluid Mech.* 177: 265–292
- Schadow S C, Gutmark E J 1992 *Prog. Energy Combust. Sci.* 18: 117–132
- Sivasegaram S, Whitelaw J H 1987 *Combust. Sci. Technol.* 52: 413–426
- Sterling J D, Zukoski E E 1991 *Combust. Sci. Technol.* 77: 225–238
- Yu K H, Trouve A C, Daily J W 1991 *J. Fluid Mech.* 232: 47–72